

Polycyano-Anion-Based Energetic Salts

Haixiang Gao,^[a] Zhuo Zeng,^[b] Brendan Twamley,^[b] and Jean'ne M. Shreeve*^[b]

Abstract: Energetic salts based on polycyano anions and cations with a high nitrogen content tend to have extensive hydrogen bonding and exhibit heats of formation up to $\Delta H_f = 1579.1 \text{ kJ mol}^{-1}$. Based on theoretical calculations, some of the new salts may be considered to be low-energy monopropellants. One of the salts can be used as a precursor to a carbon nitride.

Keywords: density functional calculations • energetic salts • heats of formation • heterocycles • nitriles

Introduction

The synthesis of energetic compounds has attracted considerable interest over recent years,^[1–4] especially in the synthesis and application of new members of heterocyclic-based energetic salts.^[5,6] Designing energetic materials based on combinations of different ions for a specific purpose provides a powerful methodology. The impact on properties as a function of the cations and anions and the variation of substituents on those ions obtained from earlier studies provides important knowledge.^[6]

In a recent study on the design and synthesis of novel energetic salts, we reported new energetic salts with nitrodicyanomethanide and dinitrodicyanomethanide anions paired with 1,5-diamino-4-methyltetrazolium, 1,4-dimethyl-5-aminotetrazolium, 1,4,5-trimethyltetrazolium, 1-methyl-4-amino-1,2,4-triazolium, 1,4-dimethyltriazolium, and 1,3-dimethylimidazolium cations. These salts exhibit higher standard enthalpies of formation than their nitrate analogues, mainly arising from the introduction of the cyano group.^[7] The presence of this moiety is predicted by theoretical calculations to result in an increase in the heat of formation (higher than for either the NO_2 or NF_2 groups but lower

than for the N_3 group).^[8] In the light of this finding, we sought a new anion source that contained a large number of cyano groups to design salts of higher energy. 1,1,2,3,3-Pentacyanopropene (PCP) and 2-dicyanomethylene-1,1,3,3-tetracyanopropane (DTP) are two of the strongest CH acids known.^[9] PCP and DTP salts, similar to derivatives of superacids, have been the subject of considerable interest in the field of coordination chemistry and molecular materials.^[10] These organic anions are interesting because of their ability to act in various coordination modes and for their high electronic delocalization.^[11] The PCP and DTP anions have higher heats of formation relative to the nitrodicyanomethanide and dinitrodicyanomethanide anions.^[7] However, to date, the utilization of these compounds as energetic materials has been limited to the suggestion of using some metal salts of DTP in propellant compositions.^[12]

Herein, we report the synthesis and calculated heats of formation of energetic salts based on the PCP and DTP anions. One of the salts can be used as a precursor to a carbon nitride.

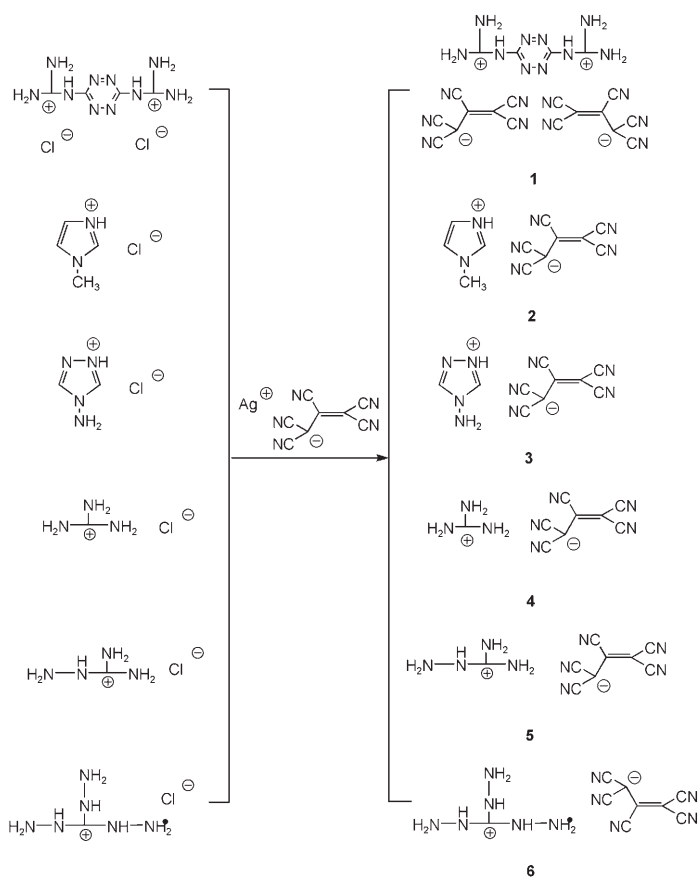
Results and Discussion

The synthesis of energetic salts **1–6** and **8–10** was accomplished by treating silver PCP salts (Scheme 1) or barium DTP salts (Scheme 2) with stoichiometric amounts of guanidine, aminoguanidine, or nitrogen-rich bases as chloride or sulfate salts. Attempts to recrystallize **6** from acetone gave the condensation product with the triaminoguanidine cation, thus leading to salt **7** (Scheme 3), the cation of which was previously reported only as its iodide.^[13] All of the salts were isolated as highly crystalline materials in excellent yields with good purity. Differential scanning calorimetry (DSC) and thermogravimetric analysis (TGA) support the

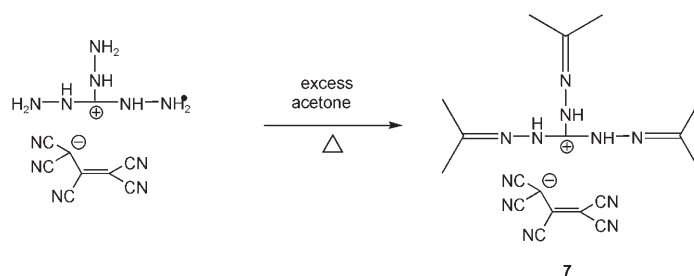
[a] Dr. H. Gao
Department of Applied Chemistry
China Agricultural University
Beijing, China 100094

[b] Dr. Z. Zeng, Dr. B. Twamley, Prof. Dr. J. M. Shreeve
Department of Chemistry
University of Idaho, Moscow
Idaho, 83844–2343 (USA)
Fax: (+1) 208-885-9146
E-mail: jshreeve@uidaho.edu

Supporting information for this article is available on the WWW under <http://www.chemeurj.org/> or from the author.



Scheme 1. Synthesis of PCP salts.

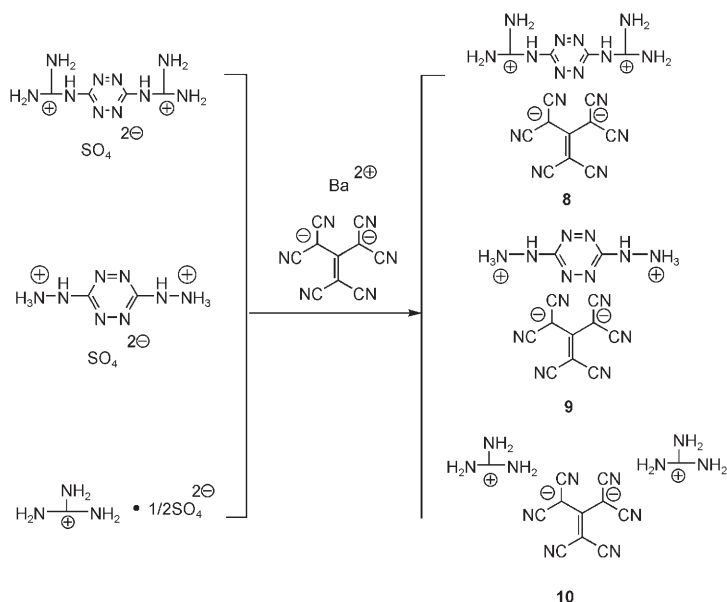


Scheme 3. Schiff base of the triaminoguanidinium PCP salt

Phase-transition temperatures (midpoints of melting points T_m) for all the salts were determined by DSC studies (Table 1), and all the salts have melting points greater than 100 °C. Their decomposition temperatures were determined by TGA studies and, with the exception of **3**, **7**, and **9**, decompose well above 200 °C. Salt **10** has the highest thermal stability and decomposes at 354.1 °C.

The heats of formation (kJ mol^{-1} and kJ g^{-1}) for **1–6** and **8–10** were calculated (Table 1). The molar heat of formation of **1** is $\Delta H_f = 1579.1 \text{ kJ mol}^{-1}$, which exceeds the values for **2** and **6** and is probably because of the high heat of formation of the cation. This value is the highest calculated for any compound in this study. Interestingly, although salt **9** comprises the cation and anion with the two highest heats of formation presented herein, the higher lattice energy results in a heat of formation considerably lower than that of **1**, although the cation is common to both. Although the DTP anion has a higher heat of formation than the PCP anion, the heat of formation of **8** is much lower than that of **1**, even with a common cation. It is obvious that the higher lattice energy and lower number of anions in **8** counteract the influence of the heat of formation of the anion. The same phenomenon is also found with **4** and **10**, which have essentially the same molar heats of formation. Therefore, one must be mindful of both the influence of the ions and the lattice energy when designing new energetic salts. The heats of formation of all the salts are reported in kJ g^{-1} and were calculated (Table 1). Salts **4**, **6**, and **9** have the highest energy densities (2.66, 3.39, and 3.16 kJ g^{-1} , respectively) and have higher values than the energy densities of known salts with a high nitrogen content (i.e., for guanidinium 5,5'-azotetrazolate (**11**), triaminoguanidinium 3,6-bisnitroguanilyl-tetrazine (**12**), and triaminoguanidinium 5,5'-azotetrazolate (**13**) the energy densities are 1.44, 2.54, and 2.87 kJ g^{-1} , respectively,^[6m,o] Scheme 4).

Calculation of detonation properties and specific impulse I_{sp} values using Cheetah 4.0 shows that salt **9** has the highest detonation pressure ($P = 14.66 \text{ GPa}$) and velocity ($\nu D = 6856 \text{ ms}^{-1}$) comparable to that of 2,4,6-trinitrophenyl-*N*-methylnitramine (tetryl; $P = 14.2 \text{ GPa}$, $\nu D = 6680 \text{ ms}^{-1}$).^[14] All of the salts with the exception of **2** have higher detonation velocities than some energetic salts, such as mercury fulminate, lead azide, silver azide, lead styphnate, and ammonium nitrate ($\nu D = 4250, 4630, 4000, 5200,$ and 5270 ms^{-1} , respectively).^[14c] Moreover, several of the salts



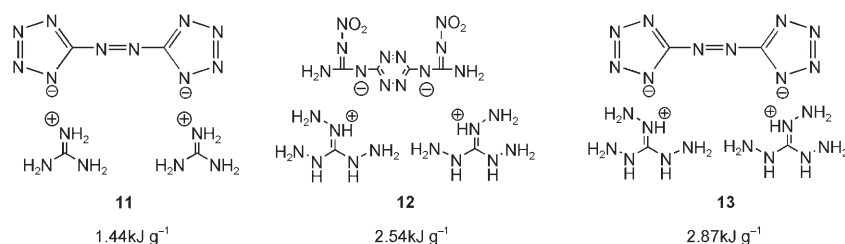
Scheme 2. Synthesis of DTP salts.

existence of a new family of very stable salts that decompose well above their relatively high melting points. This behavior can most likely be attributed to the high thermal stability of the PCP or DTP anions in the salts.

Table 1. Properties of energetic PCP and DTP salts.

Salt	$d^{[a]}$ [g cm ⁻³]	$T_m^{[b]}$ [°C]	$T_d^{[c]}$ [°C]	$\Delta H_f^{[d]}$ (cation) [kJ mol ⁻¹]	$\Delta H_f^{[d]}$ (anion) [kJ mol ⁻¹]	Lattice energy ^[d] [kJ mol ⁻¹]	ΔH_t [kJ mol ⁻¹]	ΔH_t [kJ g ⁻¹]	$P^{[e]}$ [GPa]	$\nu D^{[f]}$ [ms ⁻¹]	$I_{sp}^{[g]}$ [s]
1	1.43	–	261.4	1903.6	494.9	1314.3	1579.1	2.98	9.98	5816	162.8
2	1.29	124.8	223.0	680.6	494.9	451.5	724.0	2.90	6.41	4892	151.9
3	1.37	133.0	194.1	936.3	494.9	457.5	973.7	3.88	9.51	5718	181.3
4	1.37	–	221.4	575.9	494.9	469.9	600.9	2.66	9.11	5600	157.6
5	1.41	148.6	233.1	667.4	494.9	465.6	696.7	2.89	11.19	6104	168.8
6	1.36	113.6	221.6	871.5	494.9	447.9	918.5	3.39	12.39	6400	189.4
7	1.21	129.3	197.9	–	–	–	–	–	–	–	–
8	1.50	134.8	258.8	1903.6	668.3	1806.3	765.6	1.90	11.01	6154	144.5
9	1.55	–	188.7	2302.0	668.3	1871.0	1099.3	3.16	14.66	6856	175.3
10	1.41	–	354.1	575.9	668.3	1194.2	625.8	1.92	11.03	6131	154.7

[a] Density. [b] Melting point. [c] Decomposition temperature. [d] Heat of formation. [e] Detonation pressure. [f] Detonation velocity. [g] Specific impulse.



Scheme 4. Nitrogen-rich salts.

(i.e., **1**, **3**, **5**, **6**, and **9**) with I_{sp} values of > 160 s may be classified in the low-energy monopropellant class (Table 1).

After the decomposition by TGA of **8**, a brown porous powder remained in the pan. To obtain a larger amount of material, 4.9 mg of **8** was heated to 350 °C under nitrogen to yield 3.6 mg of porous carbon nitride, which was characterized by IR spectroscopic and elemental analysis and scanning electron microscopy (SEM; Figure 1). The results indicate that the porous powder is a carbon nitride. Elemental analysis shows the product to have the formula of CN_{0.73}H_{0.37}. The IR spectrum of carbon nitride is given in Figure 2 and is dominated by absorption bands in the region 950–1800 cm⁻¹, which are consistent with conjugated C=N and C=C species (1600–1700 cm⁻¹) and N=N bonds

(1253 cm⁻¹). The product shows only a minor absorption near 2200 cm⁻¹, which is the region in which the cumulated double-bond (N=N=N or N=C=N) and triple-bond (C≡N) absorptions lie.^[15] The spectrum obtained using SEM analysis shows that the carbon nitride materials formed a glassy microstructure with large holes and voids (Figure 1a). At

higher magnification, a fused spherical particle morphology is evident on the surface of the solid (Figure 1b). Carbon nitrides are of current interest as a result of their novel mechanical, optical, and tribological properties, which include low density, surface roughness, wear resistance, chemical inertness, and biocompatibility.^[16]

Prior reports indicate that precursors to carbon nitrides are neutral compounds, such as triazine derivatives^[15,16e,f,17] and polyazide compounds.^[18] It appears that energetic salts were not decomposed to carbon nitrides, but rather azide-containing compounds, which are sensitive to temperature and friction, were used. Our salts have higher thermal stabilities and lower friction sensitivities and provide a new route to the synthesis of carbon nitrides.

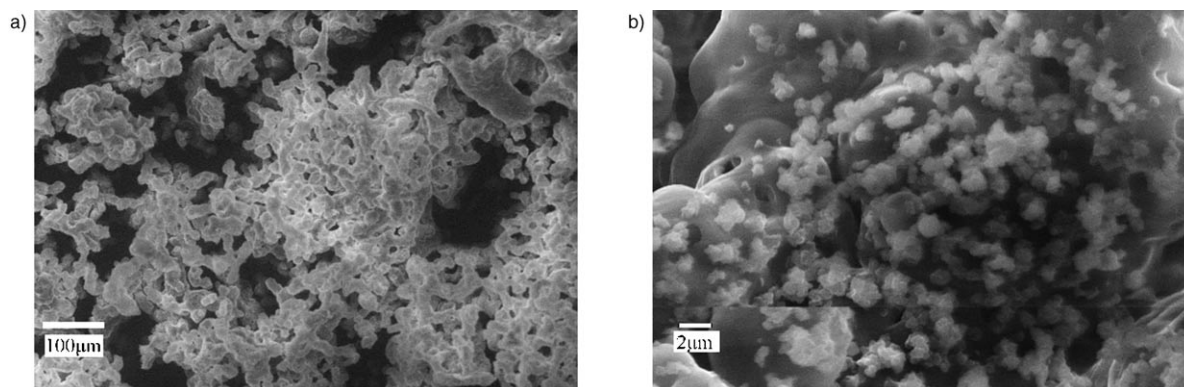
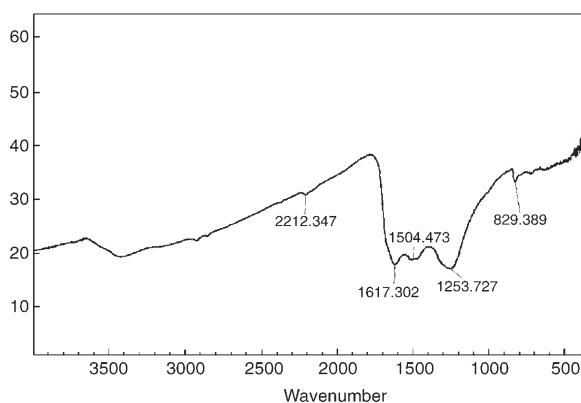


Figure 1. SEM images of amorphous carbon nitride at magnifications of a) 135× and b) 3500×.

Figure 2. IR spectrum of a carbon nitride prepared from salt **8**.

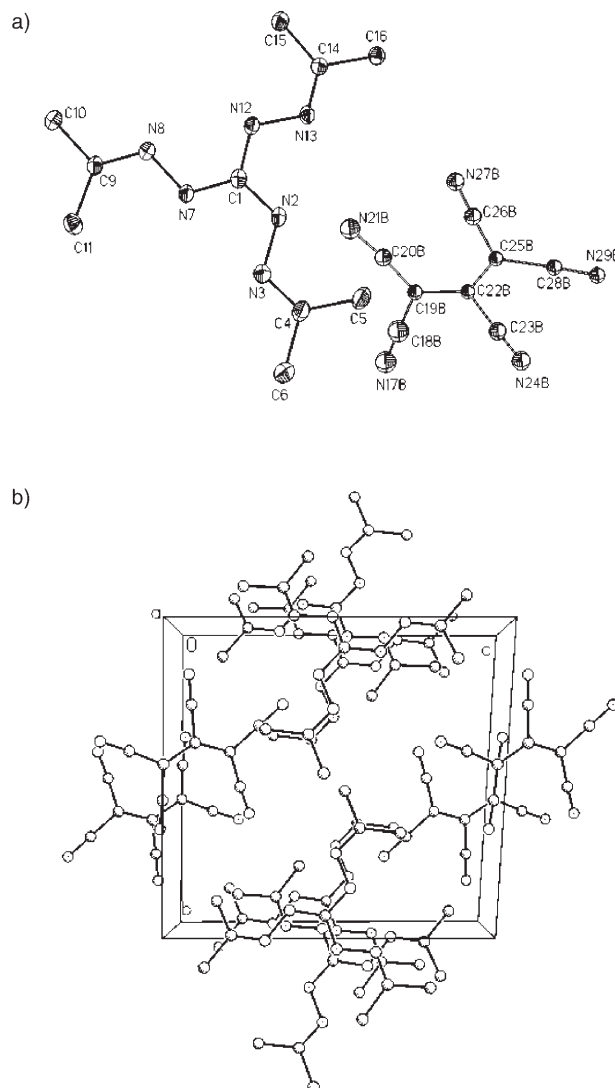
X-ray crystallography: Crystals of both samples suitable for X-ray diffraction were obtained by slow evaporation from acetone for **7** and aqueous solution for **8** (Table 2). The ion pair in **7** is symmetry unique, whereas the cation and anion in **8** lie on the inversion centre and the full structure, including lattice H₂O molecules, is generated by symmetry. The cation core and anion in **7** are essentially planar, thus indicating delocalization of the charge. The PCP anion exists in two disordered orientations (inverted to each other) with

Table 2. Crystallographic data and structure-refinement parameters.

	7	8
formula	C ₁₈ H ₂₁ N ₁₁	C ₁₄ H ₁₄ N ₁₆ O ₂
<i>M_w</i>	391.46	438.41
crystal system	triclinic	monoclinic
space group	<i>P</i> 1	<i>C</i> 2/ <i>c</i>
<i>a</i> [Å]	7.6298(4)	11.874(2)
<i>b</i> [Å]	11.7947(7)	13.426(2)
<i>c</i> [Å]	12.1206(7)	13.112(3)
<i>α</i> [°]	91.550(2)	90
<i>β</i> [°]	91.235(2)	106.477(3)
<i>γ</i> [°]	107.647(3)	90
<i>V</i> [Å ³]	1038.53(10)	2004.5(6)
<i>Z</i>	2	4
<i>T</i> [K]	90(2)	90(2)
<i>λ</i> [Å]	0.71073	0.71073
<i>ρ</i> _{calcd} [Mg m ⁻³]	1.252	1.453
<i>μ</i> [mm ⁻¹]	0.084	0.109
<i>F</i> (000)	412	904
crystal size [mm ³]	0.25 × 0.24 × 0.08	0.37 × 0.12 × 0.07
<i>θ</i> range [°]	1.68–25.25	2.35–25.24
index ranges	−9 ≤ <i>h</i> ≤ 9 −14 ≤ <i>k</i> ≤ 14 −14 ≤ <i>l</i> ≤ 14	−14 ≤ <i>h</i> ≤ 14 −16 ≤ <i>k</i> ≤ 16 −15 ≤ <i>l</i> ≤ 15
number of reflections collected	15050	15168
number of independent reflections	3754	1813
<i>R</i> (int)	0.0238	0.0373
data/restraints/param.	3754/0/319	1813/12/174
GOF	1.026	1.020
<i>R</i> ₁ (<i>I</i> > 2σ(<i>I</i>)) ^[a]	0.0462	0.0317
<i>wR</i> ₂ (<i>I</i> > 2σ(<i>I</i>)) ^[a]	0.1122	0.0715
largest differential peak, hole [e Å ⁻³]	0.351, −0.219	0.215, −0.183
CCDC reference	651004	651005

$$[a] R_1 = \frac{\sum \|F_o\| - \sum \|F_c\|}{\sum \|F_o\|}; wR_2 = \left\{ \frac{\sum [w(F_o^2 - F_c^2)^2]}{\sum [w(F_o^2)^2]} \right\}^{1/2}$$

the majority position (82%; Figure 3 a). The charge delocalization in the disordered PCP anion is also reflected in similar bond lengths to propene (C19–C22–C25: 1.389(4),

Figure 3. a) Displacement ellipsoid plot (30%) of **7** showing numbering scheme. The disordered anion is shown in the most occupied conformation. b) Ball-and-stick diagram of the extended structure of **7** viewed down the *a* axis. The hydrogen atoms are omitted for clarity.

1.382(3) Å; C19b–C22b–C25b: 1.45(2), 1.42(1) Å). There is only weak hydrogen bonding between the ion pair in the extended structure of **7** (C11...N29: 3.492(8); C15...N17: 3.300(4) Å; Figure 3b). There is, however, strong intramolecular hydrogen bonding around the cation triskelion (N2...N13: 2.601(2); N7...N3: 2.631(2); N12...N8: 2.632(2) Å), which also stabilizes the charge.

The dication in the centrosymmetric dimer **8** (Figure 4a) is also essentially planar, which again indicates delocalization of the charge. This delocalization is also displayed in the shortened bond lengths of C5–N (C5–N6: 1.319(2); C5–N7: 1.306(2); C5–N4: 1.365(2) Å), which are similar to the

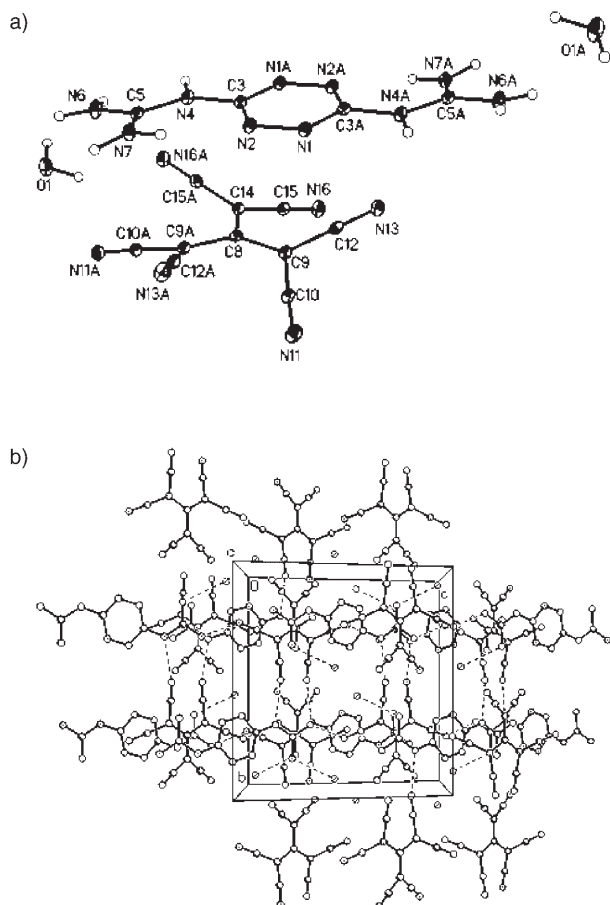


Figure 4. a) Displacement ellipsoid plot (30%) of **8**. The hydrogen atoms are included but unlabeled for clarity. b) Ball-and-stick packing diagram of **8** viewed down the *a* axis. The dashed lines indicate hydrogen bonding. Hydrogen atoms are omitted for clarity.

bond lengths of diguanidinium hexafluorosilicate, for example.^[19] The anion shows remarkable homogenization of bond lengths throughout, but instead of a planar arrangement assumes a propeller twist of approximately 17–21° around the central C8 atom. Charge delocalization is further assisted by hydrogen bonding directly between the cation and anion (N6··N13: 2.916(2); N6··N11: 3.203(2) Å) and also by the lattice water molecules (O1··N13: 3.103(2); O1··N16: 3.071(2) Å). The complex 3D structure is built up from hydrogen-bonded sheets with the water molecules occupying voids that are parallel to the *a* axis (Figure 4b). Structural characterization of these types of anions is rare, and there is only one other report of a DTP salt.^[20] The anion in this quinolinium salt also has a propeller twist with the dicyano groups at approximately 13 and 24° to the central carbon atom.

Theoretical study: To obtain a better understanding of the PCP and DTP anions, a natural bond orbital (NBO) population analysis fixed at the optimized structures ((HF/6-31+G(d,p) and DFT/6-31+G(d,p)) was used to investigate the bonding and hybridization in this species (single-point

energy calculated at the HF/6-311++G(3df,2p) and DFT/6-311++G(3df,2p) levels).^[21] The calculations were carried out using a Gaussian 03 (Revision D.01) suite of programs.^[22] The geometric optimization of the structures and frequency analyses was carried out using B3-LYP functional with the 6-31+G** basis set,^[23] and the single-point energy was calculated at the MP₂(full)/6-311++G** level. All of the optimized structures were characterized to be true local energy minima on the potential-energy surface without imaginary frequencies. The NBO analysis (Figure 5 and

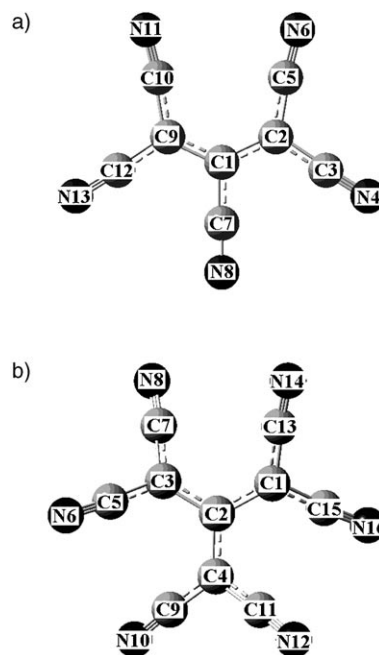


Figure 5. PCP and DTP anions (NBO analysis).

Tables 3 and 4) showed that the optimized free anion has a symmetric charge distribution for the PCP (C2=C9, C3=C12, N4=N13, C5=C10, N6=N11) and DTP (C1=C3=C4, C5=C7=C9=C11=C13=C15, N6=N8=N10=N12=N14=N16) anions, and the negative charge is delocalized over the nitrogen and carbon atoms in the cyano groups.

Table 3. NBO charge distribution of the PCP anion.

Atom	Hartree-Fock ^[a]		DFT ^[b]	
	Mulliken	NBO	Mulliken	NBO
C1	0.136	0.092	0.523	-0.033
C2,C9	0.648	-0.443	0.848	-0.360
C3,C12	0.947	0.353	0.500	0.295
N4,N13	-1.342	-0.412	-1.110	-0.365
C5,C10	0.750	0.345	0.363	0.289
N6,N11	-1.284	-0.388	-1.053	-0.341
C7	0.731	0.312	0.484	0.290
N8	-1.305	-0.313	-1.102	-0.292

[a] HF/6-31+G(d,p)//HF/6-311++G(3df,2p). [b] B3LYP/6-31+G(d,p)//B3LYP/6-311++G(3df,2p).

Table 4. NBO charge distribution of the DTP anion.

Atom	Hartree-Fock ^[a]		DFT ^[b]	
	Mulliken	NBO	Mulliken	NBO
C1,C3,C4	0.250	-0.550	0.667	-0.451
C2	-0.0640	0.283	0.0356	0.131
C5,C7, C9, C11,C13, C15	0.959	0.401	0.494	0.326
N6, N8,N10, N12, N14, N16	-1.406	-0.506	-1.167	-0.456

[a] HF/6-31+G(d,p)//HF/6-311++G(3df,2p). [b] B3LYP/6-31+G(d,p)//B3LYP/6-311++G(3df,2p).

Based on a Born-Haber energy cycle (Figure 6), the heat of formation of a salt can be simplified by the expression (I):

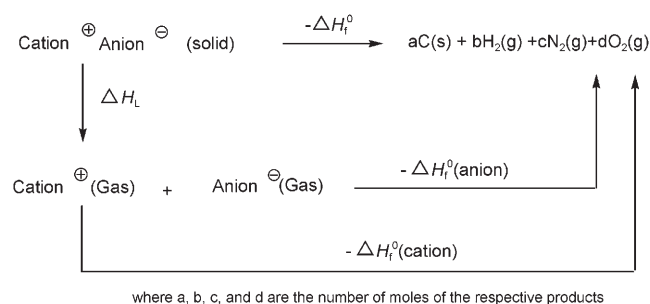


Figure 6. Born-Haber cycle for the formation of energetic salts.

$$\Delta H_f^\circ(\text{ionic salt, 298 K}) = \Delta H_f^\circ(\text{cation, 298 K}) + \Delta H_f^\circ(\text{anion, 298 K}) - \Delta H_L \quad (\text{I})$$

where ΔH_L is the lattice energy of salt M_pX_q , which could be predicted by the expression (II) suggested by Jenkins et al.^[24] as:

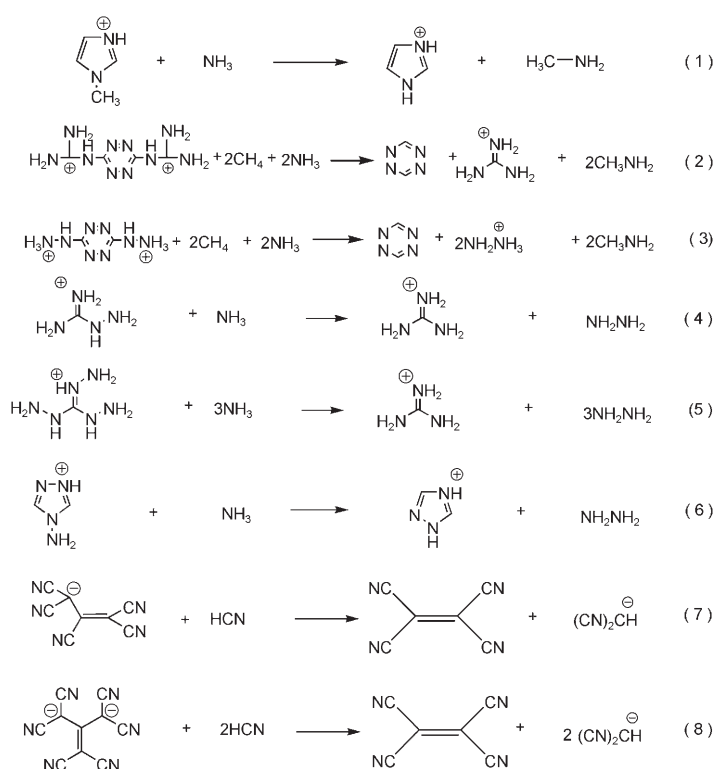
$$\Delta H_L = U_{\text{pot}} + [p(n_M/2-2) + q(n_X/2-2)]RT \quad (\text{II})$$

where n_M and n_X depend on the nature of the ions M^{q+} and X^{p-} (q and p are the charges on the cation and anion), respectively, and are equal to 3 for monatomic ions, 5 for linear polyatomic ions, and 6 for nonlinear polyatomic ions. The equation for lattice potential energy U_{pot} (given in kJ mol^{-1}) has the form (III):

$$U_{\text{POT}} = \gamma(\rho_m/M_m)^{1/3} + \delta \quad (\text{III})$$

where ρ_m is the density (g cm^{-3}), M_m is the chemical formula mass of the ionic material (g or mg), and the coefficients γ ($\text{kJ mol}^{-1} \text{cm}$) and δ (kJ mol^{-1}) take their values from previous reports.^[8,26]

The remaining task was the determination of the heats of formation of the cations and anions, which was computed by using the method of isodesmic reactions (Scheme 5). The sources of the energies of the parent ions in the isodesmic reactions were calculated from protonation reactions ($\Delta H_f^\circ(\text{H}^+) = 1530 \text{ kJ mol}^{-1}$; Scheme 5).^[8,25] The enthalpy of



Scheme 5. Isodesmic reactions of ions.

an isodesmic reaction ($\Delta H_r^\circ_{298}$) is obtained by combining the MP2(full)/6-311++G** energy difference for the reaction, the scaled zero-point energies (B3LYP/6-31+G**), and other thermal factors (B3LYP/6-31+G**). The heats of formation of the cations and anions being investigated can then be extracted readily (see the Supporting Information).

Conclusion

The formation of salts based on polycyano anions provides a straightforward approach to energetic salts that exhibit physical properties, such as relatively high thermal stabilities ($T_d > 198^\circ\text{C}$) and high heats of formation. Some salts have specific-impulse characteristics that identify them as low-energy monopropellants, and one of these salts can be used as a precursor for a carbon nitride.

Experimental Section

Caution: While we have experienced no difficulties with the shock and friction sensitivity of these salts, they must be synthesized only in millimolar amounts and handled with caution.

General: All the reagents were of analytical grade, purchased from commercial sources, and used as received. Silver 1,1,2,3,3-pentacyanopropene and barium 2-dicyanomethylene-1,1,3,3-tetracyanopropanediide was prepared by using previously reported methods.^[26] 3,6-Diguanidino-1,2,4,5-tetrazine^[26,27] and 3,6-dihydrazino-1,2,4,5-tetrazine^[28] were synthesized by using previously reported methods. ¹H and ¹³C NMR spectra were re-

corded on a 300-MHz NMR spectrometer operating at 300.13 and 75.48 MHz, respectively. Chemical shifts are reported relative to Me₄Si. The solvent was deuterated dimethyl sulfoxide ([D₆]DMSO) unless otherwise specified. The melting and decomposition points were recorded on a differential scanning calorimeter (DSC) and a thermogravimetric analyzer (TGA) at a scan rate of 10 °C min⁻¹, respectively. IR spectra were recorded using KBr pellets. The densities of energetic salts were measured at room temperature using a Micromeritics Accucyc 1330 gas pycnometer. Elemental analyses were obtained on an Exeter CE-440 Elemental Analyzer. SEM images were recorded on an AMRAY 1830 scanning electron microscope.

X-ray crystallography: Crystals of **7** and **8** were removed from the flask, a suitable crystal was selected and attached to a glass fiber, and the data were collected at 90(2) K using a Bruker/Siemens SMART APEX instrument (MoK_α radiation, λ = 0.71073 Å) equipped with a Cryocool NeverIce low-temperature device. The data were measured using omega scans of 0.3° per frame for 20 s,^[5] and a full sphere of data was collected. A total of 2400 frames were collected for each structure with a final resolution of 0.83 Å. Cell parameters for **7** were retrieved by using SMART^[29] software and refined by using SAINTPlus^[30] on all observed reflections. For **8**, cell parameters were retrieved by using APEX2^[31] software and refined by using the INTEGRATE module^[32] on all observed reflections. Data reduction and correction for Lorentzian polarization and decay were performed by using the SAINTPlus software. Absorption corrections were applied by using SADABS.^[33] Structures were solved by direct methods and refined by the least-squares method on F² using the SHELXTL program package.^[34] The structure of **7** was solved in the space group P1 (no. 2) by analysis of systematic absences. The anion was disordered (82:18) and the minor moiety was held to be isotropic. All other non-hydrogen atoms were refined anisotropically. The structure of **8** was solved in the space group C2/c (no. 15) by analysis of systematic absences. All non-hydrogen atoms were refined anisotropically. No decomposition was observed during data collection for either sample. Some restraints were applied in both models to stabilize atomic displacements. Details of the data collection and refinement are given in Table 2.

Synthesis

3,6-Biguanidinetetrazine pentacyanopropenide (1): Silver pentacyanopropenide (274 mg, 1 mmol) and 3,6-biguanidinetetrazine hydrochloride (136 mg, 0.5 mmol) were suspended in water (10 mL). After the mixture had been stirred at 50 °C for 3 h, the solids were removed by filtration, the solvent was removed slowly, and the product isolated as red needles (189 mg, 71 %). IR (KBr pellet): $\tilde{\nu}$ = 3421, 3338, 3190, 3082, 3010, 2927, 2449, 2206, 1698, 1645, 1604, 1559, 1490, 1421, 1294, 1074, 1033, 941, 747, 646, 531 cm⁻¹; ¹H NMR: δ = 8.15 (s, br) ppm; ¹³C NMR: δ = 159.7, 155.5, 136.2, 117.7, 115.3, 114.6, 55.4 ppm; elemental analysis (%) calcd for C₂₀H₁₀N₂₀ (530.43): C 45.29, H 1.90, N 52.81; found: C 45.13, H 1.78, N 52.24.

Methylimidazolium pentacyanopropenide (2): Silver pentacyanopropenide (274 mg, 1 mmol) was suspended in water (10 mL) and an aqueous solution of 1,2,3-methylimidazolium chloride (119 mg, 1 mmol) was added. After the mixture had been stirred at room temperature for 3 h, the solids were removed by filtration, the solvent was removed slowly, and the product isolated as yellow needles (214 mg, 86 %). IR (KBr pellet): $\tilde{\nu}$ = 3147, 3024, 2974, 2444, 2367, 2198, 1995, 1640, 1579, 1546, 1428, 1380, 1300, 1143, 1006, 906, 821, 771, 666, 626, 530 cm⁻¹; ¹H NMR: δ = 8.98 (s, 1H), 7.61 (s, 1H), 7.58 (s, 1H), 3.86 (s, 3H) ppm; ¹³C NMR: δ = 137.1, 136.2, 124.4, 121.0, 117.7, 115.3, 114.6, 58.4, 36.8 ppm; elemental analysis (%) calcd for C₁₂H₇N₇ (249.23): C 57.83, H 2.83, N 39.34; found: C 57.55, H 2.59, N 39.59.

4-Aminotriazolium pentacyanopropenide (3): Silver pentacyanopropenide (274 mg, 1 mmol) was suspended in water (10 mL) and an aqueous solution of 4-aminotriazolium chloride (121 mg, 1 mmol) was added. After the mixture had been stirred at room temperature for 3 h, solids were removed by filtration, the solvent was removed slowly, and the product isolated as yellow plates (201 mg, 80 %). IR (KBr pellet): $\tilde{\nu}$ = 3327, 3237, 3136, 3011, 2843, 2455, 2211, 1995, 1718, 1633, 1490, 1406, 1327, 1249, 1207, 1042, 1002, 933, 869, 670, 613, 530, 496 cm⁻¹; ¹H NMR: δ = 9.51 (s, 2H), 9.50 (s, br, 2H) ppm; ¹³C NMR: δ = 145.2, 136.2, 117.7,

115.3, 114.6, 58.4 ppm; elemental analysis (%) calcd for C₁₀H₅N₉ (251.21): C 47.81, H 2.01, N 50.18; found: C 47.52, H 1.87, N 49.86.

Guanidinium pentacyanopropenide (4): Silver pentacyanopropenide (274 mg, 1 mmol) was suspended in water (10 mL) and an aqueous solution of guanidine chloride (95 mg, 1 mmol) was added. After the mixture had been stirred for 3 h, the solids were removed by filtration, the solvent was removed slowly, and the product isolated as yellow needles (201 mg, 89 %). IR (KBr pellet): $\tilde{\nu}$ = 3460, 3275, 3199, 2449, 2208, 1659, 1570, 1504, 1385, 1153, 975, 613, 530, 499 cm⁻¹; ¹H NMR: δ = 6.83 (s) ppm; ¹³C NMR: δ = 159.3, 136.2, 117.7, 115.3, 114.6, 58.5 ppm; elemental analysis (%) calcd for C₉H₆N₈ (226.20): C 47.79, H 2.67, N 49.54; found: C 47.62, H 2.38, N 49.02.

Aminoguanidinium pentacyanopropenide (5): Silver pentacyanopropenide (274 mg, 1 mmol) was suspended in water (10 mL) and an aqueous solution of aminoguanidine chloride (111 mg, 1 mmol) was added. After the mixture had been stirred for 3 h, the solids were removed by filtration, the solvent was removed slowly, and the product isolated as yellow plates (171 mg, 71 %). IR (KBr pellet): $\tilde{\nu}$ = 3477, 3382, 3269, 2874, 2694, 2459, 2229, 2218, 1987, 1628, 1508, 1385, 1248, 1196, 1004, 968, 916, 668, 516, 481, 467 cm⁻¹; ¹H NMR: δ = 8.47 (s, 1H), 7.09 (s, 2H), 6.72 (s, 2H), 4.57 (s, 2H) ppm; ¹³C NMR: δ = 160.1, 136.2, 117.7, 115.3, 114.6, 58.5 ppm; elemental analysis (%) calcd for C₉H₇N₉ (271.24): C 44.81, H 2.93, N 52.26; found: C 44.70, H 2.75, N 51.85.

1,2,3-Triaminoguanidinium pentacyanopropenide (6): Silver pentacyanopropenide (274 mg, 1 mmol) was suspended in water (10 mL) and an aqueous solution of 1,2,3-triaminoguanidine chloride (141 mg, 1 mmol) was added. After the mixture had been stirred for 3 h, the solids were removed by filtration, the solvent was removed slowly, and the product isolated as yellow plates (203 mg, 75 %). IR (KBr pellet): $\tilde{\nu}$ = 3381, 3329, 3220, 2874, 2762, 2207, 1986, 1915, 1681, 1605, 1500, 1435, 1385, 1346, 1195, 1130, 1054, 948, 754, 668, 639, 569, 530, 464, 450, 403 cm⁻¹; ¹H NMR: δ = 8.58 (s, 3H), 4.48 (s, 6H) ppm; ¹³C NMR: δ = 160.4, 136.2, 118.3, 115.3, 114.6, 58.4 ppm; elemental analysis (%) calcd for C₉H₉N₁₁ (271.24): C 39.85, H 3.34, N 56.80; found: C 39.80, H 3.12, N 56.67.

Tris[methylidene(methylidene)amino]guanidinium pentacyanopropenide (7): 1,2,3-Triaminoguanidinium pentacyanopropenide (136 mg, 0.5 mmol) was dissolved in acetone (5 mL). After the mixture had been stirred at 45 °C for 0.5 h, the solvent was removed slowly and the product isolated as yellow plates (177 mg, 95 %). Yellow crystals suitable for X-ray diffraction were obtained upon recrystallization from acetone. IR (KBr pellet): $\tilde{\nu}$ = 3317, 3002, 2955, 2921, 2196, 1992, 1634, 1509, 1437, 1379, 1338, 1261, 1095, 1038, 673, 613, 510, 469 cm⁻¹; ¹H NMR: δ = 9.22 (s, 3H), 2.14 (s, 9H), 2.05 (s, 9H) ppm; ¹³C NMR: δ = 162.3, 150.2, 136.4, 118.1, 115.1, 114.4, 58.2, 25.2, 17.6 ppm; elemental analysis (%) calcd for C₁₈H₂₁N₁₁ (391.43): C 54.95, H 5.89, N 39.16; found: C 55.08, H 5.23, N 39.53.

3,6-Diguanidino-1,2,4,5-tetrazine 2-dicyanomethylene-1,1,3,3-tetracyanopropanediide (8): Barium 2-dicyanomethylene-1,1,3,3-tetracyanopropanediide (172 mg, 0.5 mmol) and 3,6-biguanidinetetrazine sulfate (149 mg, 0.5 mmol) were suspended in water (10 mL). After the mixture had been stirred at 50 °C for 3 h, the solids were removed by filtration, the solvent was removed slowly, and the product isolated as dark red needles (164 mg, 81 %). Dark red crystals suitable for X-ray diffraction were obtained upon recrystallization from water. IR (KBr pellet): $\tilde{\nu}$ = 3522, 3010, 2822, 2488, 2433, 2180, 2119, 1972, 1708, 1649, 1608, 1397, 1296, 1128, 1035, 943, 879, 856, 765, 655, 592, 534, 472 cm⁻¹; ¹H NMR: δ = 8.15 (s, br) ppm; ¹³C NMR: δ = 172.3, 161.9, 155.5, 121.9 ppm; elemental analysis (%) calcd for C₁₄H₁₀N₁₆·2H₂O (438.37): C 38.36, H 3.22, N 51.12; found: C 38.09, H 3.02, N 50.86.

3,6-Dihydrazinetetrazine 2-dicyanomethylene-1,1,3,3-tetracyanopropanediide (9): Barium 2-dicyanomethylene-1,1,3,3-tetracyanopropanediide (172 mg, 0.5 mmol) and 3,6-bihydrazinetetrazine sulfate (120 mg, 0.5 mmol) were suspended in water (10 mL). After the mixture had been stirred at 50 °C for 3 h, the solids were removed by filtration, the solvent was removed slowly, and the product isolated as dark-red plates (147 mg, 84 %). IR (KBr pellet): $\tilde{\nu}$ = 3489, 3133, 2683, 2189, 1701, 1606, 1558, 1420, 1325, 1213, 1176, 1105, 941, 879, 850, 570, 535, 460 cm⁻¹; ¹H NMR: δ = 10.63 (s, br) ppm; ¹³C NMR: δ = 166.1, 162.5, 122.9 ppm; elemental analy-

sis (%) calcd for $C_{12}H_8N_{14} \cdot H_2O$ (366.30): C 39.35, H 2.75, N 53.53; found: C 38.84, H 2.55, N 53.09.

Guanidinium 2-dicyanomethylene-1,1,3,3-tetracyanopropanediide (10): Barium 2-dicyanomethylene-1,1,3,3-tetracyanopropanediide (172 mg, 0.5 mmol) was suspended in water (10 mL) and an aqueous solution of 1,2,3-triaminoguanidine chloride (216 mg, 1 mmol) was added. After the mixture had been stirred for 3 h, the solids were removed by filtration, the solvent was removed slowly, and the product isolated as yellow needles (146 mg, 90%). IR (KBr pellet): $\tilde{\nu}$ = 3457, 3357, 3264, 3200, 2827, 2191, 2171, 2122, 1664, 1482, 1426, 1143, 883, 684, 532, 503, 481 cm^{-1} ; 1H NMR: δ = 6.83 (s) ppm; ^{13}C NMR: δ = 166.2, 159.4, 122.1 ppm; elemental analysis (%) calcd for $C_{12}H_{13}N_{12}$ (325.31): C 44.30, H 4.03, N 51.67, found: C 44.37, H 3.61, N 51.31.^[35]

Acknowledgements

The authors gratefully acknowledge the support of HDTRA1-07-1-0024, NSF (CHE-0315275), and ONR (N00014-06-1-1032). The Bruker (Siemens) SMART APEX diffraction facility was established at the University of Idaho with the assistance of the NSF-EPSCoR program and the M.J. Murdock Charitable Trust (Vancouver, Canada).

- [1] a) M. Goebel, T. M. Klapötke, *Z. Anorg. Allg. Chem.* **2007**, *633*, 1006–1017; b) H. Gao, C. Ye, O. D. Gupta, J. C. Xiao, M. A. Hiskey, B. Twamley, J. M. Shreeve, *Chem. Eur. J.* **2007**, *13*, 3853–3860; c) H. Xue, H. Gao, B. Twamley, J. M. Shreeve, *Chem. Mater.* **2007**, *19*, 1731–1739; d) T. Hawkins, L. Hall, K. Tollison, A. Brand, M. McKay, G. W. Drake, *Propellants, Propellants Explos. Pyrotech.* **2006**, *31*, 196–204.
- [2] a) A. Hammerl, T. M. Klapötke, M. Warchhold, *Propellants Explos. Pyrotech.* **2003**, *28*, 163–173; b) D. E. Chavez, M. A. Hiskey, R. D. Gilardi, *Angew. Chem.* **2000**, *112*, 1861–1863; *Angew. Chem. Int. Ed.* **2000**, *39*, 1791–1793; c) D. E. Chavez, M. A. Hiskey, R. D. Gilardi, *Org. Lett.* **2004**, *6*, 2889–2891.
- [3] A. Hammerl, T. M. Klapötke, M. Warchhold, *Inorg. Chem.* **2001**, *40*, 3570–3575.
- [4] a) Y. Ou, B. Chen, J. Li, H. Jia, *Heterocycles* **1994**, *38*, 1651–1664; b) K. Y. Lee, J. E. Kennedy, B. W. Asay, S. F. Son, E. S. Martin, *AIP Conference Proceedings*, Springer, New York, **2004**, vol. 706 (Part 2, Shock Compression of Condensed Matter), pp. 855–858; c) J. C. Bottaro, R. J. Schmitt, M. A. Petrie, P. E. Penwell, U. S. Patent 6,255,512, **2001**; d) M. S. Pevzner, *Russ. Chem. J.* **1997**, *41*, 73–81; e) O. P. Shitov, V. L. Korolev, V. S. Bogdanov, V. A. Tartakovsky, *Russ. Chem. Bull.* **2003**, *52*, 695–699.
- [5] a) G. Drake, T. Hawkins, A. Brand, L. Hall, M. McKay, A. Vij, I. Ismail, *Propellants Explos. Pyrotech.* **2003**, *28*, 174–180; b) G. Kaplan, G. Drake, K. Tollison, L. Hall, T. Hawkins, *J. Heterocycl. Chem.* **2005**, *42*, 19–27; c) G. W. Drake, T. M. Hawkins, J. Boatz, L. Hall, A. Vij, *Propellants Explos. Pyrotech.* **2005**, *30*, 156–163.
- [6] a) H. Xue, Y. Gao, B. Twamley, J. M. Shreeve, *Chem. Mater.* **2005**, *17*, 191–198; b) H. Xue, S. W. Arritt, B. Twamley, J. M. Shreeve, *Inorg. Chem.* **2004**, *43*, 7972–7977; c) Y. Gao, S. W. Arritt, B. Twamley, J. M. Shreeve, *Inorg. Chem.* **2005**, *44*, 1704–1712; d) C. F. Ye, J. M. Shreeve, *Chem. Commun.* **2005**, 2570–2572; e) H. Xue, Y. Gao, B. Twamley, J. M. Shreeve, *Inorg. Chem.* **2005**, *44*, 5068–5072; f) H. Xue, B. Twamley, J. M. Shreeve, *J. Mater. Chem.* **2005**, *15*, 3459–3465; g) H. Xue, Y. Gao, B. Twamley, J. M. Shreeve, *Inorg. Chem.* **2005**, *44*, 7009–7013; h) C. M. Jin, C. F. Ye, C. Piekarski, B. Twamley, J. M. Shreeve, *Eur. J. Inorg. Chem.* **2005**, *18*, 3760–3767; i) H. Xue, H. Gao, B. Twamley, J. M. Shreeve, *Eur. J. Inorg. Chem.* **2006**, *15*, 2959–2965; j) H. Gao, C. Ye, R. W. Winter, G. L. Gard, M. E. Sitzmann, J. M. Shreeve, *Eur. J. Inorg. Chem.* **2006**, *15*, 3221–3226; k) Y. Gao, C. F. Ye, B. Twamley, J. M. Shreeve, *Chem. Eur. J.* **2006**, *12*, 9010–9018; l) H. Gao, R. Wang, B. Twamley, M. A. Hiskey, J. M. Shreeve, *Chem. Commun.* **2006**, 4007–4009; m) M. A. Hiskey, D. E. Chavez, D. L. Naud, S. F. Son, H. L. Berghout, C. A. Bolme, *Proc. Int. Pyrotech. Semin.* **2000**, *27*, 3–14; n) D. E. Chavez, M. A. Hiskey, R. D. Gilardi, *Org. Lett.* **2004**, *6*, 2889–2891; o) M. A. Hiskey, N. Goldman, J. R. Stine, *J. Energ. Mater.* **1998**, *16*, 119–127.
- [7] R. Wang, H. Gao, C. Ye, B. Twamley, J. M. Shreeve, *Inorg. Chem.* **2007**, *46*, 932–938.
- [8] M. W. Schmidt, M. S. Gordon, J. A. Boatz, *J. Phys. Chem. A* **2005**, *109*, 7285–7295.
- [9] R. H. Boyd, *J. Am. Chem. Soc.* **1961**, *83*, 4288–4290.
- [10] a) F. Thetiot, S. Triki, J. S. Pala, C. J. Gomez-Garcia, *Syn. Metals* **2005**, *153*, 481–484; b) V. A. Kaminskii, O. Y. Slabko, A. V. Kachanov, B. V. Buhvetskii, *Tetrahedron Lett.* **2003**, *44*, 139–140; c) O. O. Alekseeva, L. L. Rodina, A. V. Ryzhakov, S. M. Korneev, *Russ. J. Org. Chem.* **1997**, *33*, 1320–1331.
- [11] S. Triki, F. Thetiot, F. Vandeveld, J. Sala-Pala, C. J. Gómez-García, *Inorg. Chem.* **2005**, *44*, 4086–4093, and references therein.
- [12] V. A. Engelhardt, US Patent 3017301, **1962**.
- [13] K. N. Zelenin, A. G. Saminskaya, O. B. Kuznetsova, *Zh. Obshch. Khim.* **1996**, *66*, 141–146.
- [14] a) L. E. Fried, K. R. Glaesemann, W. M. Howard, P. C. Souers, *CHEETAH 4.0 User's Manual*, Lawrence Livermore National Laboratory, **2004**; b) J. P. Lu, *Evaluation of the Thermochemical Code, CHEETAH 2.0 for Modelling Explosives Performance*, DSTO-TR-1199, DSTO, Edinburgh, **2001**; c) P. W. Cooper, *Explosives Engineering*, Wiley-VCH, New York **1996**.
- [15] B. V. Lotsch, W. Schnick, *Chem. Mater.* **2006**, *18*, 1891–1900.
- [16] a) F. Z. Cui, D. J. Li, *Surf. Coat. Technol.* **2000**, *131*, 481–487, and references therein; b) W. Long, Y. Shun, Y. Bing, *Rare Met.* **2002**, *31*, 96–100, and references therein; c) E. K. Wilson, *Chem. Eng. News* **2004**, *82*, 34–35, and references therein; d) E. Kroke, M. Schwarz, *Coord. Chem. Rev.* **2004**, *248*, 493–532, and references therein; e) D. R. Miller, J. Wang, E. G. Gillan, *J. Mater. Chem.* **2002**, *12*, 2463–2469; f) J. Wang, D. R. Miller, E. G. Gillan, *Chem. Commun.* **2002**, 2258–2259.
- [17] a) C. Li, X. Yang, B. Yang, Y. Yan, Y. Qian, *Mater. Chem. Phys.* **2007**, *103*, 427–432; b) T. C. Mu, J. Huang, Z. M. Liu, B. X. Han, Z. H. Li, Y. Wang, T. Jiang, H. Gao, *J. Mater. Res.* **2004**, *19*, 1736–1741; c) C. Li, C. B. Cao, H. S. Zhu, *Mater. Lett.* **2004**, *58*, 1903–1906.
- [18] M. H. V. Huynh, M. A. Hiskey, J. G. Archuleta, E. L. Roemer, *Angew. Chem.* **2005**, *117*, 747–749; *Angew. Chem. Int. Ed.* **2005**, *44*, 737–739; J. Wang, E. G. Gillan, *Thin Solid Films* **2002**, *422*, 62–68; E. G. Gillan, *Chem. Mater.* **2000**, *12*, 3906–3912.
- [19] A. Waskowska, *Acta Crystallogr. Sect. A* **1997**, *C53*, 128–130.
- [20] S. Sakanoue, N. Yasuoka, N. Kasai, M. Kakudo, *Bull. Chem. Soc. Jpn* **1971**, *44*, 1–8.
- [21] E. D. Glendening, A. E. Reed, J. E. Carpenter, F. Weinhold, NBO Version 3.1, as implemented in Gaussian 03, Revision, D.01, Gaussian, Inc., Wallingford, CT, **2004**.
- [22] M. J. Frisch, G. W. Trucks, H. B. Schlegel, G. E. Scuseria, M. A. Robb, J. R. Cheeseman, J. A. Montgomery, Jr., T. Vreven, K. N. Kudin, J. C. Burant, J. M. Millam, S. S. Iyengar, J. Tomasi, V. Barone, B. Mennucci, M. Cossi, G. Scalmani, N. Rega, G. A. Petersson, H. Nakatsuji, M. Hada, M. Ehara, K. Toyota, R. Fukuda, J. Hasegawa, M. Ishida, T. Nakajima, Y. Honda, O. Kitao, H. Nakai, M. Klene, X. Li, J. E. Knox, H. P. Hratchian, J. B. Cross, V. Bakken, C. Adamo, J. Jaramillo, R. Gomperts, R. E. Stratmann, O. Yazyev, A. J. Austin, R. Cammi, C. Pomelli, J. W. Ochterski, P. Y. Ayala, K. Morokuma, G. A. Voth, P. Salvador, J. J. Dannenberg, V. G. Zakrzewski, S. Dapprich, A. D. Daniels, M. C. Strain, O. Farkas, D. K. Malick, A. D. Rabuck, K. Raghavachari, J. B. Foresman, J. V. Ortiz, Q. Cui, A. G. Baboul, S. Clifford, J. Cioslowski, B. B. Stefanov, G. Liu, A. Liashenko, P. Piskorz, I. Komaromi, R. L. Martin, D. J. Fox, T. Keith, M. A. Al-Laham, C. Y. Peng, A. Nanayakkara, M. Challacombe, P. M. W. Gill, B. Johnson, W. Chen, M. W. Wong, C. Gonzalez, J. A. Pople, *Gaussian 03, Revision D.01*, Gaussian, Inc., Wallingford CT, **2004**.
- [23] R. G. Parr, W. Yang, *Density Functional Theory of Atoms and Molecules*, Oxford University Press, New York, **1989**.
- [24] H. D. B. Jenkins, D. Tudeal, L. Glasser, *Inorg. Chem.* **2002**, *41*, 2364–2367.

- [25] S. G. Lias, J. E. Bartmess, J. F. Liebman, J. H. Holmes, R. D. Levin, W. G. Mallard, *J. Phys. Chem. Ref. Data, Suppl. 1*, **1988**, 17.
- [26] W. J. Middleton, E. L. Little, D. D. Coffman, V. A. Engelhardt, *J. Am. Chem. Soc.* **1958**, *80*, 2795–2806.
- [27] D. E. Chavez, M. A. Hiskey, D. Naud, *Propellants Explos. Pyrotech.*, **2004**, *29*, 209–215.
- [28] D. E. Chavez, M. A. Hiskey, *J. Energ. Mater.*, **1999**, *17*, 357–377.
- [29] SMART, v. 5.630, Bruker Molecular Analysis Research Tool, Bruker AXS, Madison WI, **2001**.
- [30] SAINTPlus, v. 7.23a, Data Reduction and Correction Program, Bruker AXS, Madison WI, **2004**.
- [31] APEX2, v. 2.1–0, Bruker AXS, Madison WI, **2005**.
- [32] INTEGRATE module, SAINTPlus, v. 7.23a, Data Reduction and Correction Program, Bruker AXS, Madison WI, **2005**.
- [33] SADABS, v. 2004/1, An Empirical Absorption Correction Program, Bruker AXS, Madison WI, **2004**.
- [34] G. M. Sheldrick, SHELXTL, v. 6.14, Structure Determination Software Suite, Bruker AXS, Madison WI, **2004**.
- [35] CCDC-651004 and CCDC-651005 contain the supplementary crystallographic data for this paper. These data can be obtained free of charge The Cambridge Crystallographic Data Centre via www.ccdc.cam.ac.uk/data_request/cif. Ab initio computational data are given in the Supporting Information.

Received: July 23, 2007

Revised: September 18, 2007

Published online: November 19, 2007